Designed folding of pseudopeptides: the transformation of a configurationally driven preorganization into a stereoselective multicomponent macrocyclization

Ignacio Alfonso,*,[a] Michael Bolte,[b] Miriam Bru,[c] M. Isabel Burguete,[c] and Santiago V. Luis*,[c]

Abstract: The efficient synthesis of large ring size pseudopeptidic macrocycles through a multicomponent [2+2] reductive amination reaction is described. The reaction is completely governed by the structural information contained in the corresponding open-chain pseudopeptidic bis(amidoamine) precursors, which bear a rigid (R,R)-cyclohexane-1,2-diamine moiety. A remarkable *match/mismatch* relationship between the configurations of the chiral centers of the cyclic diamine and those of the peptidic frame is observed. The macrocyclic tetraimine intermediates have been deeply studied by NMR, CD and molecular modeling, supporting the appropriate preorganization induced by the *match* combination of the chiral centers. We have also synthesized the corresponding open-chain bis(imine) model compounds. Structural studies (NMR, CD, modeling) with these systems showed an intrinsic lower reactivity of the *mismatch* combination, even when the product of the reaction is acyclic. Besides, there is a synergistic effect of both chiral substructures for the correct folding of the molecules. Finally, X-ray analysis of the HCl salt of one of the macrocycles showed an interesting pattern. The macrocyclic rings stack in columnar aggregates leaving large interstitial channels filled with water solvated chloride anions.

Keywords: Macrocycles · peptide-like structures · conformation · preorganization · foldamers.

Introduction

Amino acid containing macrocycles[1] are important molecules due to their interesting applications in molecular recognition,[2] biomedicine[3] and materials science.[4] However, in most cases, their synthesis is hampered by the macrocyclization step, which usually requires high dilution techniques, sophisticated protecting groups or tedious purification steps.[5] One possibility to improve that process is the conformational preorganization of the linear precursors.[6] However, for the *de novo* design of a conformation leading to the intended macrocyclic ring, a detailed knowledge of the structural variables for the correct folding of the open-chain precursors is mandatory. Therefore, the concept of programmed folding arises as a key stone for the macrocyclization process.[7] In nature, the structural information implemented within a given sequence leads, under certain environmental conditions, to a functional three-dimensional structure.[8] This is often achieved by the homochirality of the monomers which form the corresponding functional biopolymers.[9] Thus, there is fundamental information in the geometrical parameters obtained by the correct combination of the configuration of the corresponding chiral centers, which is expressed when the chiral components are assembled into a larger structure.[10] During the last decades, many chemists have been fascinated by synthetic molecules with a designed preferred conformation in solution, commonly called *foldamers*.[11] Moreover, some research groups have exploited the potential of structurally designed folding for organic synthesis, especially in the macrocyclic field.[12] For the efficient formation of large rings, the reactive centers must be in a well defined spatial disposition, namely preorganized in the corresponding cyclic conformation. Therefore, the geometrical parameters of the linear precursors must be carefully tuned in order to get the correct folding, exactly like in nature. To obtain that preorganization, very intelligent approaches have been carried out using geometrical restrictions,[13] intramolecular H-bonding,[14] solvophobic interactions[15] or π-stacking contacts.[16] However, reports investigating the correlation between different combination of the configurations of the chiral centers and designed folding leading to an intended reactivity are scarce.[17]

On the other hand, we have previously synthesized new pseudopeptidic macrocycles taking advantage of the U-turn preorganization of this family of compounds in aprotic polar solvents.[18] Some of these systems displayed interesting properties as organogelators,[19] molecular receptors,[20] chemosensors[21] or molecular devices.[22] Within this research project, we envisioned the preparation of larger structures in order to expand the possibilities for the generation of a family of compounds by increasing the size and complexity of the substrates. Within this idea, the reductive amination reaction arose as an interesting alternative, as imine bonds are rigid and conformationally predictable scaffolds, very useful for macrocyclic construction.[23] To this aim, the preorganization of the linear precursor is advisable in order to obtain

[a] Dr. Ignacio Alfonso
Departamento de Química Orgánica Biológica, Instituto de Investigaciones Químicas y Ambientales de Barcelona
Consejo Superior de Investigaciones Científicas (IIQAB-CSIC)
Jordi Girona, 18-26, E-08034, Barcelona (Spain)
Fax: (+) 34 932 045 904
E-mail: iarqob@iiqab.csic.es

[b] Dr. Michael Bolte
Institut für Anorganische Chemie
J. W. Goethe-Universität Frankfurt
Max-von-Laue-Str. 7, 60438, Frankfurt/Main (Germany)

[c] Miriam Bru, Dr. M. Isabel Burguete and Prof. Dr. Santiago V. Luis
Departamento de Química Inorgánica y Orgánica, UAMOA
Universidad Jaume I/CSIC
Campus del Riu Sec, Avenida Sos Baynat, s/n, E-12071, Castellón (Spain).
Fax: (+) 34 964 728 214
E-mail: luiss@qio.uji.es

Supporting information for this article is available on the WWW under http://www.chemeurj.org/ or from the author.))

acceptable final yields of the macrocyclization reaction, as well as for avoiding side oligomerization products. Accordingly, we have recently reported the use of anion templates to promote the preorganization for the selective [2+2] cyclization.[24] This conformational trend can be alternatively controlled by the appropriate re-design of the linear precursors. Here we report a complete structural study of the configurationally driven preorganization for a highly efficient multicomponent macrocyclization process, leading to new amino acid containing large macrocycles.

Results and Discussion

Design of the macrocyclization reaction: With the aim of preparing large macrocyclic structures, we initially designed a [2+2] reductive amination reaction (Scheme 1) between a pseudopeptidic bis(amidoamine) (**1a-i**)[25] and a rigid planar aromatic dialdehyde (**2a-b**). However, reactions performed with the flexible derivatives (**1a-b**, entries 1-2 in Table 1) led to a very complicated mixture of open chain oligomers, while the corresponding [2+2] macrocycles were detected by ESI-MS only as minor products. These results indicated that the ethylenediamide moiety behaves too flexible in MeOH to preorganize the system in a macrocycle-producing folded conformation.
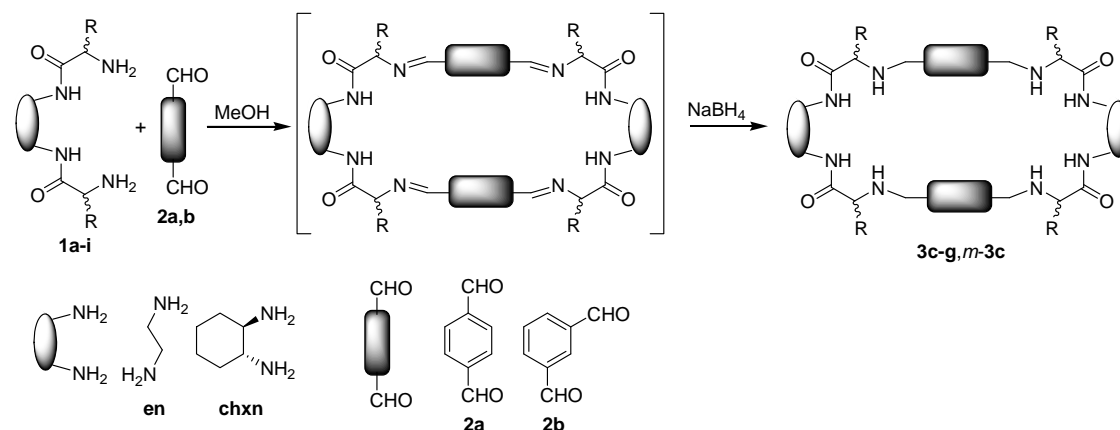
Scheme 1.

After some preliminary molecular modeling, we decided to prepare the corresponding derivatives bearing a cyclohexane-1,2-diamine moiety, which was selected in order to favor a rigid and well defined spatial disposition of the bis(amidoamine) fragment. Chiral cyclohexane-1,2-diamine had been previously used as scaffold for cyclization processes. Its chair-like conformation with the C-N bonds forming 60° has served as an excellent scaffold for the construction of large conformationally restricted macrocycles and pincers. Thus, this diamine can undergo either [2+2] or [3+3] cyclocondensation reactions,[26] generate a dynamic covalent system[27] or induce important constraints when forming part of an open-chain longer molecule.[28] In our pseudopeptidic molecules, the cyclohexane frame would induce a turn conformation in the linear precursors, thus favoring the [2+2] cyclization process. Satisfyingly, the macrocyclization reaction proceeded very nicely with these re-designed systems. Thus, aldehyde-amine condensation between **1c** and therephthaldehyde **2a** (MeOH, RT, 20 h) led to the macrocyclic tetraimine, which was *in situ* reduced with sodium borohydride to the corresponding macrocyclic tetraamine **3c** (R = iPr) in very good overall yield (entry 3, Table 1). In order to check the generalization

of the procedure, we changed other fragments of the cyclic structure in a modular way (Table 1). All the final compounds were fully characterized by NMR and mass spectrometry (See Supporting Information). Due to the D_2 averaged symmetry of the final macrocycle and to the broadness of the signals in the NMR spectra for most of the derivatives, the accurate ESI-TOF spectra were especially illustrative as an unambiguous proof of the [2+2] macrocyclic structure. Besides, we were able to get suitable crystals for X-ray diffraction analysis of one derivative **3d** (R = Bn, see last section of this paper). Comparison of the data gathered in Table 1 shows that the reaction can be performed with different aliphatic or aromatic side chains of the amino acid precursor, leading to comparable final yields (Table 1, entries 4, 6 and 7). The use of the *meta* dialdehyde (**2b**) instead of the *para* derivative decreased the isolated yield, being the rest of the material recovered as the starting compound or as open chain oligomers (entry 5). This result suggests that the geometrical disposition around the flat and rigid aromatic spacer is also important, most likely as a consequence of the higher symmetry of *para* compared to *meta* substitution of the aromatic dialdehyde. An example bearing H-bonding side chains was also obtained (derived from glutamine, entry 8 in Table 1), although only in moderate (non-optimized) yield. However, it must be pointed out that the isolation of the final compound **3g** was highly hampered by its very low solubility in most organic solvents.

We also decided to study the effect of the different combination of chiral centers of the linear pseudopeptidic bis(amidoamine) in this macrocyclization reaction. Thus, compounds **1h-i** having (*R,R*) configuration in the cylohexane moiety but D configuration in the amino acid α carbon were prepared and assayed. Very interestingly, for this combination of stereocenters, the reaction led to a mixture of compounds detected by ^{1}H NMR, TLC and ESI-MS, where the major ones corresponded to the starting material (entries 9 and 10). This means that there is a cooperative relationship of the chiral centers of the liner molecules which play a fundamental role in the macrocyclization reaction. Thus, we obtained a positive (*match*) combination with (*R,R*)-cyclohexane and L amino acids and, correspondingly, a negative (*mismatch*) combination with D amino acids. Therefore, a high diastereoselectivity was obtained for the macrocyclization reaction. Since we found these results quite intriguing, we decided to go deeply in the study of the intimate mechanism of the reaction, by characterizing the corresponding tetraimine intermediates.

**Table 1.** Multi-component reductive amination synthesis of pseudopeptidic macrocycles.

Sust.	diamine	R (Cα-conf.)	dial.	prod.	Yield[a]
1	1a	en	iPr (*S*)	2a	3a	_[b]
2	1b	en	CH₂Ph (*S*)	2a	3b	_[b]

2

3	1c	(R,R)-chxn	iPr (S)	2a	3c	67
4	1d	(R,R)-chxn	CH$_2$Ph (S)	2a	3d	55
5	1c	(R,R)-chxn	iPr (S)	2b	m-3c	35
6	1e	(R,R)-chxn	iBu (S)	2a	3e	58
7	1f	(R,R)-chxn	sec-Bu (S)	2a	3f	41
8	1g	(R,R)-chxn	(CH$_2$)$_2$CONHTr (S)	2a	3g	17[c]
9	1h	(R,R)-chxn	iPr (R)	2a	3h	–[b]
10	1i	(R,R)-chxn	CH$_2$Ph (R)	2a	3i	–[b]

[a]Isolated yield (%) after chromatographic purification. [b]Yield not determined because a complicated mixture of compounds were obtained by both ESI-MS and TLC. [c]Non-optimized yield due to the insolubility of the final compound 3g.

**Structural studies of the macrocyclic tetraimine intermediates:** In order to get more precise information about the reaction course, we followed (^{1}H NMR, 500 MHz, CD$_3$OD, 303 K) the formation of the tetraimine intermediate precursor for 3c (see Supporting Information). The reaction started just a few minutes after mixing 1c and 2a. This was indicated by the gradual disappearance of the aldehyde CHO signals (δ 9.99-10.11 ppm) and the growing of imino methyne signals (δ 8.07-8.34 ppm). In the first stage of the reaction, a complicated group of signals was formed which simplified after 24 hours. At that point, a major compound (ca. 70 % from integration of the signals) was obtained with a highly symmetrical geometry, as shown by both ^{1}H and ^{13}C NMR signals (see Supporting Information for gCOSY, TOCSY and ^{1}H-^{13}C gHSQC spectra). This major imine compound showed one singlet for the aromatic protons, which can be explained either by a fast rotation of the aromatic ring with respect to the macrocyclic main plane, or by a D_2 symmetrical conformation in solution. Regarding the relative disposition between imine bonds, they must be all in the same S-*trans* configuration or again in a fast equilibrium between S-*cis* and S-*trans* to render the observed D_2 symmetry in the NMR timescale. The presence of other minor imino signals (overall accounting for an additional ~25%) and the fact that no other cyclic compounds were isolated after reduction suggest that this minor non-symmetrical imino groups came from the presence of different relative dispositions between C=N double bonds and supports the assumption that the major compound is an all-S-*trans* isomer. All these imino signals also showed strong NOE effects with the CαH protons of the peptidomimetic moiety (Supporting Information for 2D NOESY), supporting the connectivity between both substructures, and a *syn* disposition between these protons in the major species, as depicted in Figure 1.
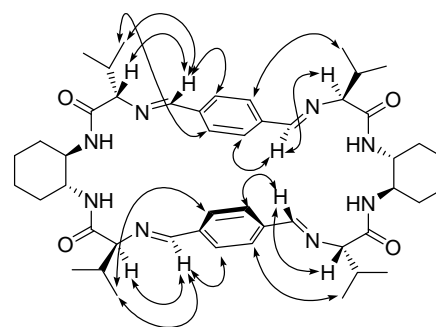
Figure 1. Observed NOEs on the macrocyclic tetraimine intermediate obtained upon condensation between 1c and 2a.

Despite that, the large geometrical preference for the system to form the D_2 symmetrical cyclic structure is highly remarkable. The composition of this mixture does not change over a long period of time (>8 weeks) or by heating the sample up to 60 ºC, supporting that it is an equilibrium mixture under thermodynamic control. It is also noteworthy that performing the same experiment with 1h (derived from D-valine) instead of 1c (derived from L-valine) led to a very complicated group of signals in the ^{1}H NMR and to the incomplete consumption of dialdehyde 2a even for very long reaction times (>3 days, Supporting Information). This is also a solid proof for the *match/mismatch* effect of the configurations of the chiral centers.

The formation of the tetraimine intermediate has been also studied by electronic circular dichroism (CD).[29] The CD of a mixture of 1c and 2a, after 24 h of reaction time, clearly showed a bisigned (−,+) curve (black line in Figure 2) with a minimum at 296 nm (Δε = −110 cm^2·mmol^{-1}) and a maximum at 269 nm (Δε = 132 cm^2·mmol^{-1}). The CD bisigned signal crosses the cero at 280 nm which is the λ$_{max}$ (ε = 59600 M^{-1}·cm^{-1}) of the UV absorbance (Figure 2). This UV band can be assigned to π-π* transitions of the aromatic diimine.[30] The CD spectrum unambiguously implies a negative split-Cotton effect, which allowed us to know the disposition of the chromophores in solution, as the dipole moment associated to the π-π* transition in this chromophore is known.[30] The magnitude of the amplitude is in agreement with a highly chiral and ordered structure setting the corresponding chromophores, namely the aromatic diimines, in a close proximity one to each other. Besides, for an appropriate comparison, we prepared the corresponding (R,R)-cyclohexane-1,2-bis(benzylimine) [(R,R)-4], and its CD spectrum was measured in the same conditions (dotted line in Figure 2). This compound showed a very similar split-Cotton effect of negative sign (−,+), although at a lower wavelength due to lesser conjugation of the chromophores. All these data imply that the chirality and the geometrical disposition of the (R,R)-cyclohexane-1,2-diamine has been efficiently transferred throughout the whole system for the macrocyclic tetraimine formed by the reaction between 1c and 2a. Even more interestingly, the corresponding experiment with the *mismatch* combination of stereocenters (1h + 2a) yielded a less intense CD spectrum (grey line in Figure 2) with no signs of exciton-coupling. These results highlight the relevance of the configurationally driven preorganization for the correct folding of the system.

3
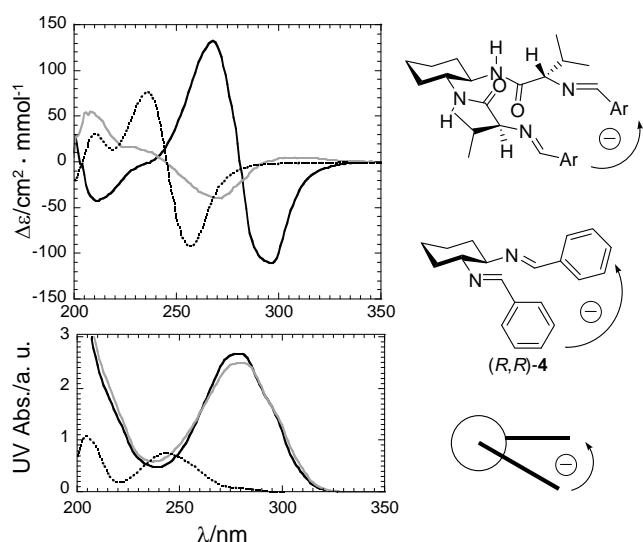
Figure 2. CD (up) and UV (down) spectra of the reactions between: **1c** + **2a** (black), **1h** + **2a** (grey) and (*R*,*R*)-**4** (dotted).

We have also performed some molecular modeling studies in order to visualize these effects. Thus, Monte Carlo conformational searches with MMFF minimizations were performed for the proposed macrocyclic tetraimines derived from either **1c** (*match*) or **1h** (*mismatch*) pseudopeptides (Figure 3). Interestingly, the cyclic compound with the *match* relationship rendered a global minimum showing a structure in a very good agreement with the experimental data (Figure 3A). It shows an average D_2 symmetry, with interatomic distances compatible with the observed NOE contacts. The cyclohexanes are in a perfect chair conformation with the substituents in equatorial positions. The structure presents an all *S-trans* relative disposition of imine bonds and a flat conformation for the aromatic diimine groups, maximizing the conjugation of the system. The isopropyl side chains set on equatorial position, pointing out of the macrocyclic structure. Besides, superposition of the energetically accessible local minima (Figure 3B) showed a rigid averaged oval shape, with slight changes in the dispositions of the side chains but retaining the conformation of the macrocyclic backbone. However, the same calculations performed with the hypothetical macrocycle derived from **1h**, with the *mismatch* configurations, rendered very different results. The macrocycle showed an averaged distorted geometry with a large number of structurally different accessible minima (Figure 3C). Most of them showed the cyclohexane moiety in a highly strained boat conformation and/or the iPr group in pseudoaxial position, which must be energetically demanding. Actually, the global minimum of this system (**1h**) is much less stable (6.58 kcal/mol) than the diastereomer derived from **1c**. All these theoretical results also support the disfavored formation of the macrocycle with the *mismatch* configurations, as observed experimentally. Besides, as the system is under thermodynamic control, these theoretical calculations must reflect a reliable picture of the process.
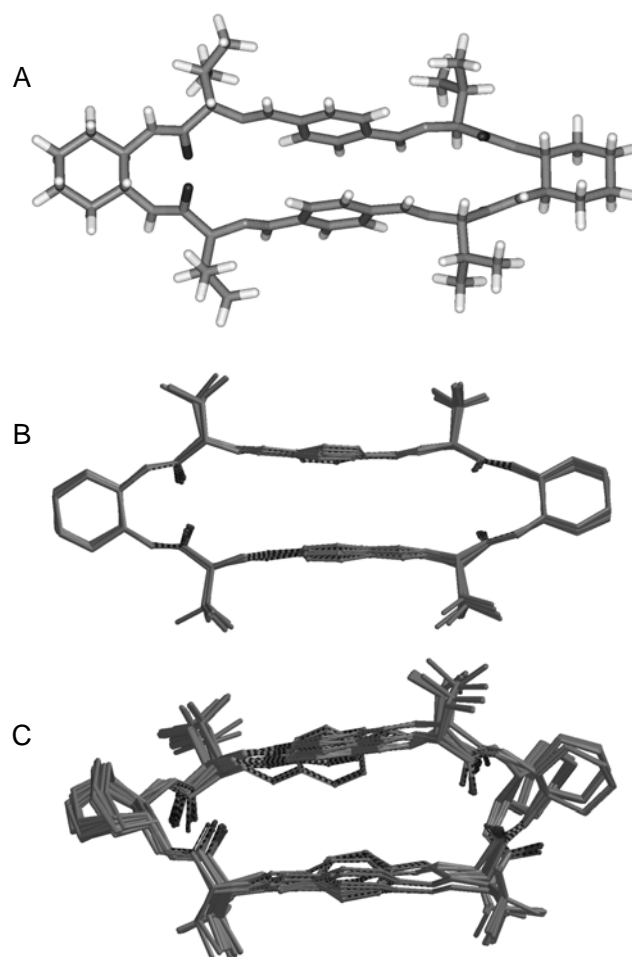
Figure 3. (A) Minimized geometry for the macrocyclic tetraimine leading to **3c**. (B,C) Superposition of the energetically accessible (≥1% from a Botzmann distribution) local minima (Monte Carlo searches with MMFF minimizations) of the macrocyclic tetraimines obtained from **1c** (B, *match*) or **1h** (C, *mismatch*). Hydrogen atoms have been omitted for clarity in B and C.

Open chain model systems: Taking into account the *match*/*mismatch* effect observed for the macrocyclization reaction, we wondered if that behavior is controlled by the structural differences of the pseudopeptidic repeating units. In other words, if the different reactivity depends completely on the formation of the macrocycle or maybe it is inherent to the pseudopeptidic moiety. Thus, we prepared four different open chain model compounds (**5a-d**) bearing a similar pseudopeptide-imine linkage (Figure 4). We synthesized, both the *match* (**5a**) and the *mismatch* (**5b**) combinations for the cyclohexane-derivatives, while for the flexible ethylene compounds, the two enantiomers (**5c-d**) were also prepared. The compounds were synthesized by the simple condensation between the corresponding bis(amidoamine) and benzaldehyde in methanol. Rather interestingly, the rate for the formation of the imine bond (estimated by ^{1}H NMR) was much slower for the *mismatch* combination (**5b**) than for the *match* diastereomer (**5a**). For instance, the reaction showed a 98% of imine conversion for **5a** after 23 h (10 mM, CD₃OD, 303 K) but a 78% of conversion for **5b** for the same reaction time. This last derivative required 75 h for achieving 93% of imine conversion by NMR. Accordingly, there is a difference in the reactivity of the initial diastereomeric bis(amidoamine) pseudopeptides **1c** and **1h**. Thus, the difference in the macrocyclization is not exclusively due to the different strain of

the final cyclic structure, as it is observable even for condensation reactions leading to open chain imines.
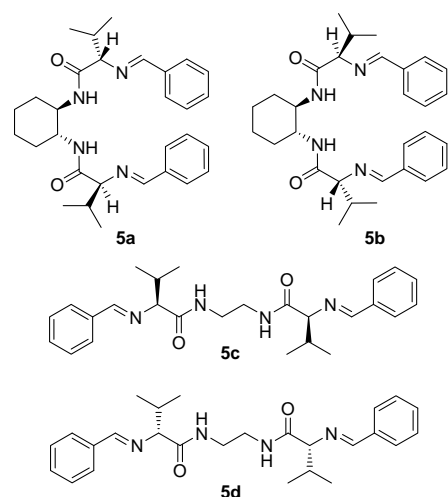

Figure 4. Open chain model systems.

The different reactivity observed for **1c**/**1h** leading to **5a**/**5b** can be rationalized considering the geometry of the possible conformations of both compounds **1c**/**1h** in solution (Scheme 2). Assuming the diequatorial positioning of the amide groups on the cyclohexane moiety and a *trans* disposition of the peptidic bonds, three different rotamers on the carbonyl-Cα bond can be proposed (conformers **I-III** in Scheme 2). According to the ^{1}H and ^{13}C NMR data, only C_2 symmetrical conformations will be considered, although other non-symmetrical geometries in dynamic equilibrium could be also present in solution. The stability, and therefore the population, of these species would depend on the stabilizing/destabilizing interactions found for every case. For instance, conformer **I** in compound **1c** would allow amide-amine N-H···N hydrogen bonding interactions, forming intramolecular five-member rings (Scheme 2a). These interactions have been previously found for related systems both in solution[18,22] and in the solid state.[18] However, this conformation (**I**) would present a large steric hindrance between isopropyl groups. On the other hand, conformer **III** of the same compound would set amide N-H and iPr groups eclipsed, accounting for a destabilizing interaction. Therefore, in polar protic solvents, conformer **II** is expected to be slightly favored for **1c**, as it would diminish steric hindrance of the iPr groups, by setting them in pseudoecuatorial positions and far away from each other. In the case of compound **1h** (Scheme 2b), the scenario would be much clearer, as two rotamers (**II** and **III**) show a steric hindrance derived from the iPr groups, while conformer **I** would have both the iPr pseudoequatorial and the proposed H-bonding stabilizing interactions. Therefore, conformer **I** should be the most populated for **1h**. By comparing both structures (**II** in **1c** versus **I** in **1h**) one can predict that the amino nitrogen atoms in **1h-I** must be less nucleophilic than those in **1c-II**, as they have their electron lone pairs implicated in intramolecular H-bonds.[31] Although MeOH would be able to break these H-bonding interactions, a clear difference in the reactivity was observed, which can be ascribed to these structural differences. Monte Carlo studies on these systems showed that conformers of the type **I** would be the most favorable for both diastereomers. This can be due to an overestimation of the H-bonding stabilization within the force field calculations (even using polar solvents such as water in the calculations). However, the

corresponding minimum for **1h** is more stable (2.16 kcal/mol) than that of **1c**, probably due to the above mentioned steric hindrance of **1c-I**. These computational results are in line with our initial hypothesis.
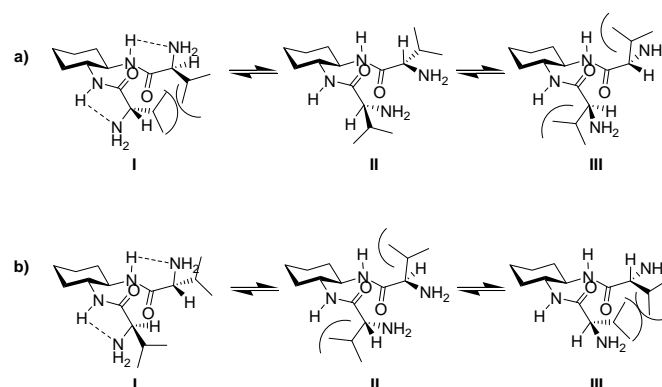
Scheme 2. Proposed conformational equilibrium for (a) **1c** and (b) **1h**.

Once the model compounds (**5a-d**) were prepared, we studied their conformation in solution. First of all, their ^{1}H NMR showed important differences relative to each other, especially in the imine-linkage region. The proton chemical shifts of **5a** are very similar to those of the flexible ethylene derivatives **5c-d** (Figure 5, Table 2, entries 1 and 6). However, compound **5b** showed a more complex group of signals, indicating the presence of at least four different imine groups. The integration of different ^{1}H NMR bands rendered a proportion of species of 80 : 14 : 3 : 2, for which some representative chemical shifts are gathered in Table 2. The minor ones (overall accounting for 19%) showed chemical shifts very similar to those of **5a** and **5c-d**. However, for the major species (80%), the protons surrounding the imine linkage shift upfield with respect to the corresponding signals of **5a** (Table 2, entries 1-2). This shielding can be only explained by the presence of a conformation setting the aromatic ring of one benzylimine group on top of the proton nuclei (aromatic imine and Cα) of the other equivalent arm, in a C-H···π disposition.
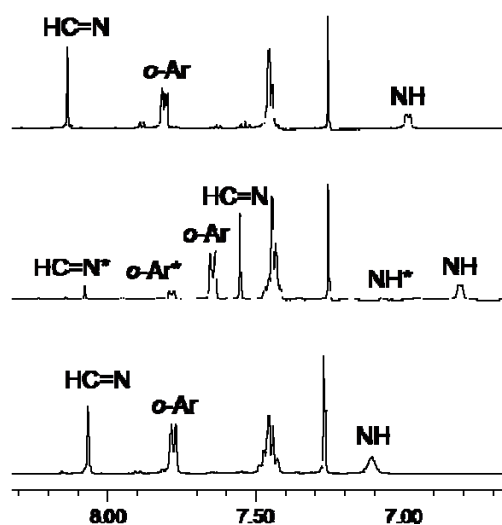

Figure 5. Selected region of the ^{1}H NMR spectra for **5a** (upper trace), **5b** (middle trace) and **5c-d** (lower trace). Signals corresponding to minor species in **5b** are shown with asterisks.

**Table 2.** Chemical shift (δ, ppm) for selected ^{1}H NMR signals of **5a-d**.

	Comp.	isomer (%)	HC=N	o-Ar-H	Cα-H	amide N-H
1	5a	n. a.	8.14	7.81	3.57	6.99
2	5b	80	7.56	7.65	3.15	6.82
3	5b	14	8.08	7.79	3.54	6.96
4	5b	3	8.15	7.84	3.60	7.19
5	5b	2	8.24	7.96	3.57	7.19
6	5c-d	n. a.	8.07	7.77	3.58	7.11

With the aim of explaining these experimental differences, we performed some molecular modeling calculations on **5a-b** (Figure 6). Monte Carlo searches on these systems supported the data obtained by NMR. Thus, **5a** behaved a bit more flexible in solution, explaining the chemical shifts similar to **5c-d**. However, **5b** seemed to be more conformationally constrained, with the accessible minima setting the protons of one aromatic imine group (namely HC=N, CαH and o-ArH) on top of the anisochrony shielding cone of the other aromatic ring (Figure 6). This disposition nicely explains the observed upfield shifts for **5b**. Although the computed geometries are not actually symmetrical, dynamic equilibrium on the NMR timescale would produce an averaged C_2 symmetry, as experimentally observed.
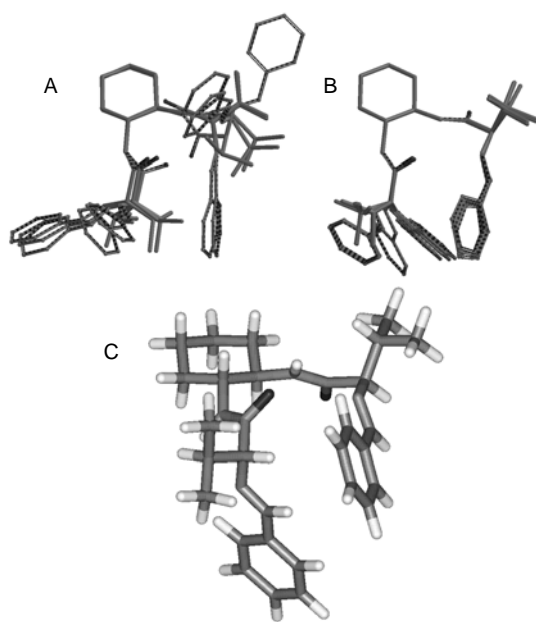

Figure 6. Superposition of the energetically accessible local minima for **5a** (A) and **5b** (B). The global minimum for **5b** is also shown (C) in a different perspective in order to highlight the disposition between aromatic imines

We additionally performed NOESY experiments with **5a-b** (Supporting Information). For the *match* diastereomeric combination, strong NOE cross-peaks were observed, in agreement with the presence of a conformation very similar to that proposed for the cyclic tetraimine intermediate (Figure 7). However, a weaker NOE effect between the amide NH and the *ortho* proton of the aromatic ring suggests the participation of other conformations with the benzylimine group in pseudoaxial position (Figure 7). The same experiment performed with **5b** was inconclusive, as the observed NOEs were those implicating imine linkage but with a much lower intensity than for **5a**.
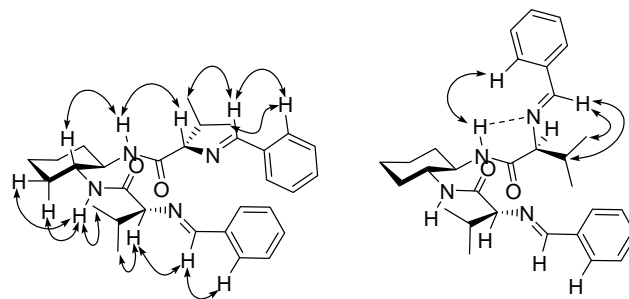
Figure 7. Observed NOEs for compound **5a**.

As a complementary technique, we also measured the CD spectra of these model compounds **5a-d** in methanol. The flexible derivative **5c** (Figure 8, black trace) showed a strong CD signal of the type (−,+,−) characterized as follows: λ_{min} = 277 nm, $\Delta\varepsilon$ = −7.5 cm^2·mmol^{-1}; λ_{max} = 244 nm, $\Delta\varepsilon$ = +20.8 cm^2·mmol^{-1}; λ_{min} = 215 nm, $\Delta\varepsilon$ = −16.0 cm^2·mmol^{-1}. As expected, its enantiomer **5d** (Figure 8, grey line) displayed a perfect mirror image (+,−,+) CD spectrum. The UV absorbance at λ_{max} = 250 nm (ε = 40000 M^{-1}·cm^{-1}) can be assigned to π-π* transitions of aromatic imine chromophores. The absence of a clear exciton-coupling effect prevented proposing a preferred conformation, but the results obtained for the macrocyclization reaction suggest that these systems are highly flexible in methanol. Therefore, these spectra can be approximately considered as the random coil CD reference.
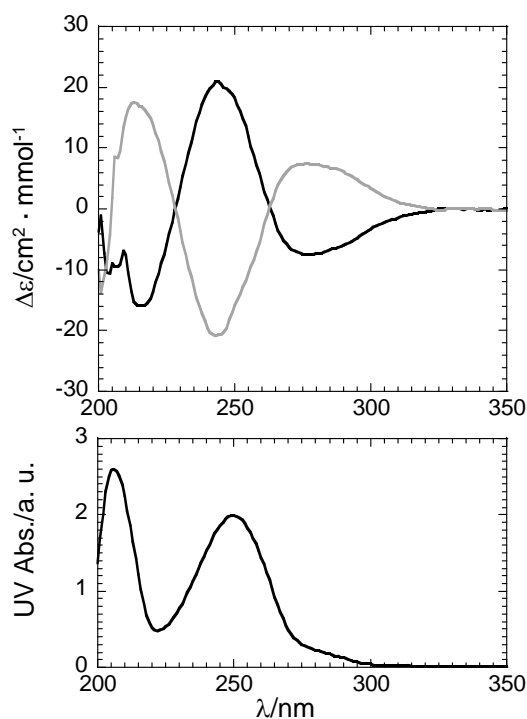
Figure 8. CD (up) and UV (down) spectra of **5c** (black) and **5d** (grey).

When measuring the corresponding CD spectra for the cyclohexane derivatives (**5a-b**), some interesting trends were obtained. First of all, for **5b** (Figure 9, grey line), the CD signal shifted to more negative values (λ_{max} = 275 nm, $\Delta\varepsilon$ = +3.7 $cm^2 \cdot mmol^{-1}$; λ_{min} = 245 nm, $\Delta\varepsilon$ = –26.9 $cm^2 \cdot mmol^{-1}$; λ_{max} = 220 nm, $\Delta\varepsilon$ = +13.7 $cm^2 \cdot mmol^{-1}$) than the corresponding reference flexible compound **5d**. Once again, no split-Cotton signal was detected, suggesting that the preorganization suitable for the macrocyclization process is not present in solution. Fortunately, CD data for **5a** were much more informative (Figure 9, black line). Comparing the CD of **5a** with the flexible derivative **5c**, the first minimum decreases its intensity (λ_{min} = 265 nm, $\Delta\varepsilon$ = –11.2 $cm^2 \cdot mmol^{-1}$), the subsequent maximum moves up in intensity (λ_{max} = 241 nm, $\Delta\varepsilon$ = +22.7 $cm^2 \cdot mmol^{-1}$) and the second minimum also goes up (λ_{min} = 215 nm, $\Delta\varepsilon$ = –14.1 $cm^2 \cdot mmol^{-1}$). A slight blue-shift of the CD was obtained as a consequence of an incipient exciton coupling effect. Besides, as the UV absorbance shows its maximum at the wavelength λ_{max} = 250 nm (ε = 34500 $M^{-1} \cdot cm^{-1}$) and the CD crosses the cero at λ_{max} = 254 nm, there must be a contribution of a bisigned exciton coupling for the π-π* transition of the aromatic imines. Besides, this split-Cotton effect clearly implies a negative chirality.
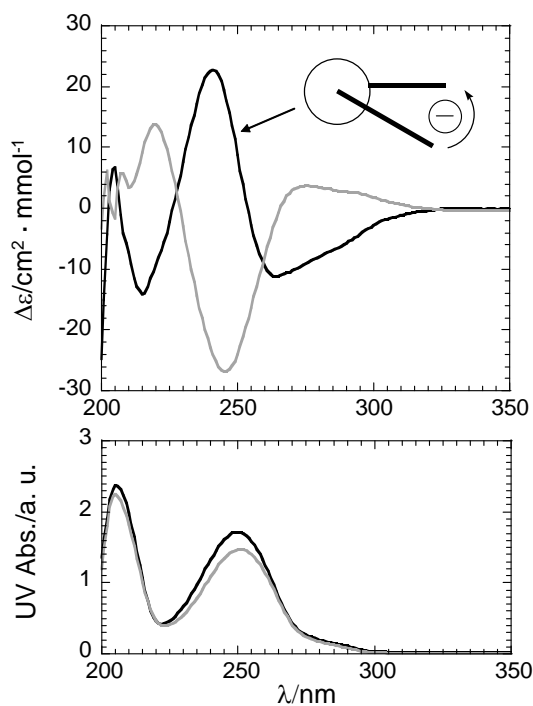
Figure 9. CD (up) and UV (down) spectra of **5a** (black) and **5b** (grey).

The negative sign of the split-Cotton effect of the imines in **5a** reflects the effective preorganization induced by the cyclohexane moiety, despite its open-chain nature. This preorganized conformation was observed in the macrocyclic tetraimine and must be the effective driving force for the [2+2] multicomponent cyclization. Moreover, we aimed to determine the contribution of every substructure (pseudopeptide and cyclohexane) in the overall preorganization.[32] To do that, we attempted to de-convolute the CD spectrum of **5a** into the corresponding two reference spectra for both substructures. Accordingly, we utilized **5c** as the reference for the pseudopeptidic contribution, while (*R,R*)-**4** (Figure 2) was used for the cyclohexane framework. Satisfyingly, we were able to reasonably reproduce the CD of **5a** (Figure 10) as a weighted

combination of both of them, rendering an approximate contribution of $\Delta\varepsilon$(**5a**) $\approx$ 0.86$\cdot\Delta\varepsilon$(**5c**) + 0.14$\cdot\Delta\varepsilon$[(*R,R*)-**4**]. Besides, the amplitude of the CD signal is inversely proportional to the square of the distance between the interacting chromophores, and that distance should be shorter for (*R,R*)-**4** than for **5a**. Thus, we are using a model sub-system with a stronger CD signature than the possible one in **5a**. Consequently, the actual conformational contribution of the cyclohexane moiety must be larger than the one calculated with our approach (14%). Anyway, this remarkable relationship can be understood as a semiquantitative expression of the *match* effect of the chiral centers on the conformational preorganization.
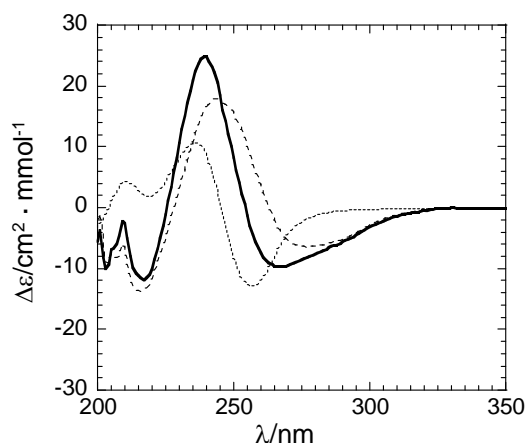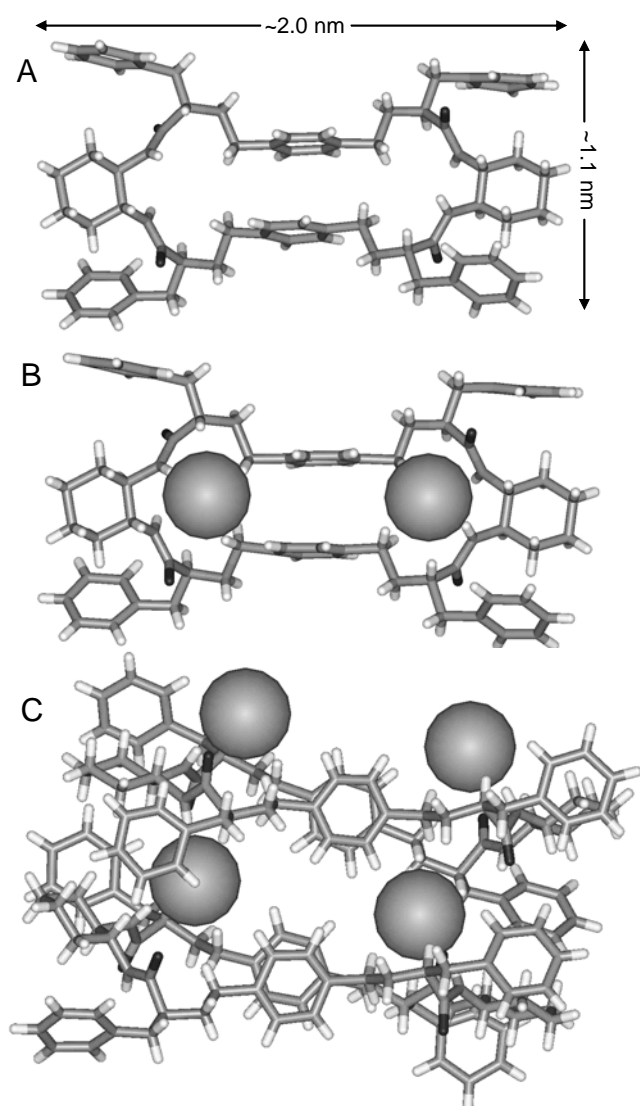

Figure 10. Simulation of the CD spectra of **5a** (black) obtained by the addition of weighted CD spectra of the corresponding substructures: 0.86$\cdot\Delta\varepsilon$ **5c** (dashed) + 0.14$\cdot\Delta\varepsilon$ (*R,R*)-**4** (dotted).

Overall, the deep structural study of the open chain model compounds rendered important conclusions regarding the *match/mismatch* effect of the chiral centers. First of all, amino nitrogens in **1c** are intrinsically more nucleophylic than those in **1h**. On the other hand, the NMR data suggests that **5a** is slightly more flexible than **5b**, as in the latter compound the disposition of the aromatic diimines in close proximity leads to some conformational constrictions. However, despite the higher flexibility of **5a**, the combination of its chiral centers make the compound to adopt a conformation suitable for macrocyclization, as demonstrated by the NOEs and CD results. More interestingly, for **5a**, we have been able to quantify the contribution of each substructure on the averaged conformation in solution. Therefore, we have demonstrated that the positive/negative preorganization for cyclization is a combination (*match/mismatch*) of both substructures, cyclohexane and peptidic, present in the molecules.

Crystal structure of 3d·4HCl: We were able to obtain crystals of the tetrahydrochloride salt of **3d**, suitable for X-Ray diffraction analysis. The results are shown in Figures 11-12. The nanometer-sized (1.1 nm x 2.0 nm) macrocycle adopts a conformation with a nearly D_2 symmetry as shown in figure 11A. The cyclohexane moiety shows a chair conformation with the amide substituents in equatorial positioning. The amide NH groups are *trans* with respect to the methynes of the chiral centers of the cyclohexane rings and *cis* to the Cα hydrogens of the peptidic fragments. The benzyl side chains are on pseudoequatorial position and pointing outwards of the macrocyclic ring. Interestingly, the aromatic rings of the side chains are folded toward the cyclohexane moieties, forming a hydrophobic core which seems to play an important role in the
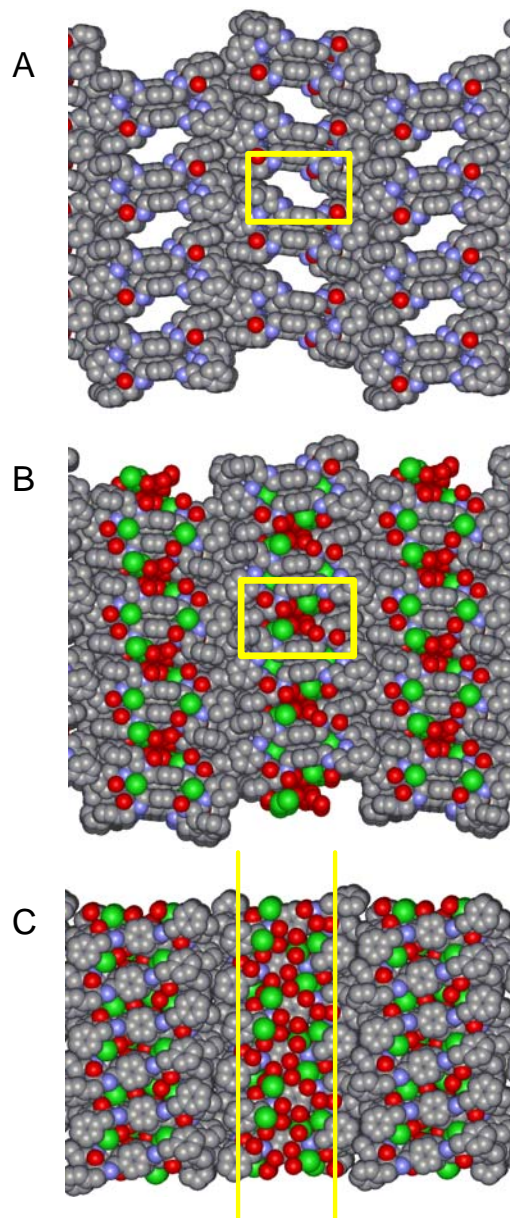
crystal packing (see below). The amino nitrogens are fully protonated and pointing outwards to the macrocycle, minimizing the mutual electrostatic repulsions. The aromatic rings of the backbone phenylene groups are perpendicular to the macrocyclic main plane and very close to each other, possibly establishing π-stacking interactions (interplanar distance ~3.6-3.7 Å). Overall, the conformation of the pseudopeptidic moiety is in good agreement with that proposed for the precursor tetraimine intermediate. The crystal has four chloride anions per macrocycle. Two of them are on top of each pseudopeptidic moiety, establishing H-bond interactions with the amide N*H* and N-C*H₂*-Ar hydrogen atoms (Figure 11B). These interactions stabilize the stacking of macrocyclic rings within a columnar supramolecular aggregation motif (figure 11C). The other two chloride atoms are outside the macrocyclic cavity rings.

between columns (see Figure 12A for the top view of empty channels). These channels have a rhomboid-shaped section with an estimated area of 92.4 Å². They are filled with chloride anions and water molecules, as the ammonium groups are pointing to the inner face of the interstitial holes, making them highly hydrophilic (Figure 12B for top view of filled channels). A longitudinal section of the channel (Figure 12C) showed an interesting pattern with solvated chloride anions along the whole funnel. Accordingly, the whole crystal structure can be alternatively described as water-filled chloride channels embedded in a hydrophobic core.

Figure 11. Top view of the macrocyclic tetracation alone (A) and with two H-bonded chloride anions (B). Side view of the columnar stacked aggregation (C) assisted by chloride anions (Chloride ions are represented in CPK model).

Figure 12. CPK representation of the crystal packing of **3d**·4HCl: upper view of interstitial channels either (A) without or (B) with chloride anions and solvent molecules; (C) longitudinal section of the chloride and water filled channels. Hydrogen atoms have been omitted for clarity (carbon: gray; nitrogen: blue; oxygen: red; chloride: green).

Conclusion

We have developed a multicomponent reductive amination macrocyclization reaction for the synthesis of new amino acid

The packing between the columnar aggregation motifs is also noteworthy. The cores formed by the benzyl side chains and the cyclohexane rings are interpenetrated, tightly packing the columns through aryl-aryl and hydrophobic contacts, on two opposite faces of the columns. The other two faces leave large interstitial channels

containing macrocycles. The efficiency of the reaction is strongly dependent on the structural parameters of the open chain pseudopeptidic bis(amidoamine) linear precursors. Moreover, the macrocyclization process is dominated by a *match/mismatch* relationship of the relative configuration of the chiral centers on both substructures: cyclic diamine and peptidic moieties. The correct combination is that having (*R,R*)-cylohexane-1,2-diamine and L amino acids. This effect has been clearly demonstrated by the study of the macrocyclic tetraimine intermediates, using different experimental (NMR, including NOEs and CD) and theoretical (Monte Carlo conformational searches) tools.

The *match/mismatch* effect on the reactivity has been further studied using the corresponding open-chain model systems. From their deep (NMR, CD and modeling) structural characterization, some important conclusions can be extracted. First of all, there is an intrinsic lower reactivity of the *mismatch* combination of the chiral centers, even for a reaction leading to open chain products. Besides, the slightly larger flexibility of the *match* diastereomer allows it to adopt the right folded conformation which leads to macrocyclization. More importantly, the CD spectra of all the model systems clearly indicates the synergistic effect of both (diamine and peptidic) substructures. For the *match* combination, this cooperative folding is expressed by a weighted participation of each conformation in the overall folding.

Finally, the crystal structure of the tetrahydrochloride of one macrocycle showed a very interesting behavior. The nanometric scaled macrocycles stack in a columnar supramolecular structure, held together with the help of H-bonding interactions with two chloride anions. These columnar entities are hydrophobically packed leaving interstitial channels filled with chloride anions and water molecules. This nice supramolecular crystal packing can be described as an anion channel inside a hydrophobic core. Anion channels are highly important entities both in chemistry[33] and in biology.[34] Our results show the potential of these simple macrocycles for preparing synthetic minimalistic chloride channels.

Experimental Section

General: General: Reagents were purchased from commercial suppliers (Adrich, Fluka or Merck) and were used without further purification. Compounds **1a-1i** were prepared following slight variations of previously reported procedures for linear diamines.[18,24] Experimental and spectroscopic details are given in the Supporting Information.

NMR spectroscopy: The NMR experiments were carried out either on a Varian INOVA 500 spectrometer (500 MHz for ^{1}H and 125 MHz for ^{13}C) or a Varian MERCURY 300 spectrometer (300 MHz for ^{1}H and 75 MHz for ^{13}C). Chemical shifts are reported in ppm using residual non-deuterated solvent peaks as internal standards.

Mass spectrometry: Mass spectra were recorded on a hybrid QTOF I (quadrupole-hexapole-TOF) mass spectrometer with an orthogonal Z-spray-electrospray interface (Micromass, Manchester, UK), or on a Micromass Quattro LC spectrometer equipped with an electrospray ionisation source and a triple-quadrupole analyzer.

Infrared spectrometry: Infrared spectra were recorded in a Perkin-Elmer 2000 FT-IR spectrometer.

CD spectroscopy: Spectra were recorded with a JASCO J-810 spectropolarimeter at RT. The normalized spectra were obtained by transforming the data in the molar circular-dichroic absortion (Δε, cm^2 · mmol^{-1}), using the formula: Δε = θ / (32980 · C · l) where θ is the measured ellipticity (in mdeg), C is the concentration (M) and l is the path-length (in cm). No changes were observed for normalized spectra at different overall concentration.

X-ray single crystal diffraction of 3d: Suitable crystals for X-ray diffraction were obtained as follows: A small amount of pseudopeptidic macrocycle **3d** (~3 mg) was dispersed in 1 mL of methanol of HPLC grade. Then, a small excess of 10% aqueous HCl was added drop wise until complete dissolution. Crystals of **3d**·4HCl were obtained by the very slow (several weeks) evaporation of the solvents. $C_{64}H_{80}N_8O_4 \cdot 4Cl^- \cdot 8H_2O$, formula weight 1311.29, orthorhombic, space group $P2_12_12_1$, a = 13.0283(15) , b = 13.0834(10) , c = 42.757(4) Å, V = 7288.1(12) Å^3, Z = 4, colorless block shaped crystal, STOE-IPDS-II -two-circle diffractometer, T = 173K, MoK$_\alpha$-radiation, 2θ-range = 3.26 – 51.36°, 26237 reflections collected, 12668 independent reflections (R_{int}= 0.1586), empirical absorption correction[35] (MULABS), structure solution with SHELXD (Sheldrick, 2008), refinement on F^2 with SHELXL-97[36], $R1$[I>2σ(I)]= 0.1215, GOF = 0.858. The absolute configuration had been determined, Flack-x-parameter = -0.06(18). All the non-hydrogen atoms were refined anisotropically. Hydrogen atoms were generated according to stereochemistry and refined using a riding model. CCDC-682038 contain the supplementary crystallographic data for this paper. These data can be obtained free of charge from the Cambridge Crystallographic Data Centre via www.ccdc.cam.ac.uk/data_request/cif.

Molecular modeling: All the theoretical calculations were performed using Spartan '06 program. The optimized geometries for the corresponding minima were obtained as follows. A stochastic conformational search was applied (Monte Carlo Search followed by MMFF force field minimization) without restrictions to each compound. More than 100 conformers were obtained in this way (ca. 10 kcal/mol cut off). The obtained structures were ordered by their energies and analyzed. The Boltzmann distributions of the corresponding conformers were calculated at 298.15 K and the superposition of the energetically accessible local minima were carried out using the same software package.

General procedure for the macrocyclization reaction, synthesis of compound 3c: Compound **1c** (160 mg, 0.512 mmol) was disolved in 5 mL of degassed CH_3OH, the solution was placed inside a flask under nitrogen. Therephthaldehyde (70 mg, 0.512 mmol) was dissolved in 3 mL of degassed CH_3OH, this solution was added over the solution of **1c** and then, 2.5 mL of CH_3OH were added until a final volume of 10.5 mL. (0.05 M final concentration each). The mixture was stirred overnight. After 20 h a large excess of NaBH$_4$ (158 mg, 4.096 mmol) was carefully added and the mixture was allowed to react for 24 h. before being hydrolyzed (conc. HCl, to acidity) and evaporated to dryness. The residue obtained was dissolved in water an basified with 1N NaOH, the product was extracted with CHCl$_3$. The combined organic layers were dried (MgSO$_4$) and the solvents were evaporated in vacuum. The product was purified by silica flash chromatography using CH_2Cl_2 as eluent while increasing slowly the polarity with MeOH, several drops of NH$_3$ were added to the mobile phase in order to improve the extraction of the product. The product was characterized as the corresponding HCl salt, prepared by addition of conc. HCl to a methanolic solution of the free amine. Yield = 67%; pale yellow solid; M.P.= It decomposes without melting over 230 °C; [α]$_D^{20}$ = +11.59 (c = 0.92, CH$_3$OH) ; IR (cm^{-1}) (KBr) 3399, 3210, 3055, 2967, 2937, 2856, 1665, 1551; ^{1}H NMR (CD$_3$OD, 500 MHz) δ (ppm) 1.06 (d, *J* = 6.8 Hz, 12H), 1.12 (d, *J* = 6.7 Hz, 12H), 1.30-1.41 (m, 8H), 1,77 (bs, 4H), 2.13 (d, *J* = 11.4 Hz, 4H), 2.29-2.36 (m, 4H), 3.83 (d, *J* = 4.9 Hz, 4H), 3.88 (bs, 4H), 4.14 (ABq, δ$_A$ = 4.10, δ$_B$ = 4.18, |*J*$_{AB}$| = 13.3 Hz, 8H), 7.60 (s, 8H), 8.52 (bs, 4H, exchangable with solvent); ^{13}C NMR (D$_2$O, 75 MHz, T = 90°C) δ (ppm) 18.1, 19.3, 25.5, 30.8, 33.9, 50.8, 53.8, 66.2, 132.4, 133.2, 167.7; ESI TOF MS (m/z) 415.5 [(M+2H)$^{2+}$100].

Compound 3d: This compound was obtained as described above starting from **1d** and therephthaldehyde, and was characterized as the corresponding HCl salt. Yield = 55%; pale yellow solid; M.P.= It decomposes without melting over 230 °C; [α]$_D^{20}$ = + 26.79 (c = 0.89, CH$_3$OH); IR (cm^{-1}) (KBr) 3402, 3048, 2935, 2856, 1668, 1557; ^{1}H NMR (CD$_3$OD, 500 MHz) δ (ppm) 0.57 (bd, *J* = 12.9 Hz, 2H), 0.68 (bs, 2H), 1.00-1.07 (m, 4H), 1.28-1.32 (m, 4H), 1.48 (bd, *J* = 8.8 Hz, 4H) 3.02 (t, *J* = 11.8 Hz, 4H), 3.45 (dd, *J*$_1$ = 13.1 Hz, *J*$_2$ = 5.0 Hz, 4H), 4.03 (dd, *J*$_1$ = 10.5 Hz, *J*$_2$ = 5.1 Hz, 2H), 4.20 (ABq, δ$_A$ = 4.15, δ$_B$ = 4.26, |*J*$_{AB}$| = 12.9 Hz, 8H), 7.25-7.35 (m, 20H), 7.69 (s, 8H); ^{13}C NMR (CD$_3$OD, 125 MHz) δ (ppm) 25.2, 33.0, 36.8, 50.3, 53.7, 63.4, 128.8, 130.0, 130.8, 132.3, 133.5, 135.4, 168.5; ESI TOF MS (m/z) 409.4 [(M+2H)$^{2+}$, 100].

Compound m-3c: This compound was obtained as described above starting from **1c** and isophthaldehyde, and was characterized as the corresponding HCl salt. Yield = 35%; pale yellow solid; M.P.= It decomposes without melting over 230 °C; [α]$_D^{20}$ = +7.63 (c = 0.375, CH$_3$OH); IR (cm^{-1}) (KBr) 3387, 3215, 3055, 1959, 2936, 2856, 1670, 1554; ^{1}H NMR (CD$_3$OD, 500 MHz) δ (ppm) 1.04-1.16 (m, 24H), 1.37-1.43 (m, 8H), 1,78 (bs, 4H), 2.11 (d, *J* = 9.7 Hz, 4H), 2.29-2.36 (m, 4H), 3.57-3.82 (m, 4H), 3.91-4.30 (m, 12H), 7.40-7.61 (m, 8H); ^{13}C NMR (CD$_3$OD, 125 MHz) δ (ppm) 18.3, 19.6, 25.4, 31.0, 33.6, 51.3, 54.1, 66.6, 131.0, 132.4, 132.9, 134.6, 168.0; ESI/MS (m/z) 415.1 [(M+2H)$^{2+}$, 100], 746.1 [(M+Na+K)$^{2+}$, 30].

Compound 3e: This compound was obtained as described above starting from **1e** and therephthaldehyde, and was characterized as free amine. Yield = 58%; white solid; M.P.= 232-237 °C; [α]$_D^{20}$ = +11.76 (c = 1.04, CHCl$_3$:CH$_3$OH 7:3); IR (cm^{-1}) (KBr) 3302, 3054, 2932, 2867, 1643, 1516; ^{1}H NMR (CDCl$_3$ with a few drops of CD$_3$OD, 500 MHz) δ (ppm) 0.81-0.84 (bt, *J* = 6.6 Hz, 24H), 1.22-1.33 (m, 12H), 1.50-1.52 (m, 8H), 1.71 (bs, 4H), 1.97 (d, *J* = 10.9 Hz, 2H), 2.08 (d, *J* = 11.8 Hz, 2H), 3.05-3.11 (m, 4H), 3.56

(ABq, δ_A = 3.59, δ_B = 3.52, |J_{AB}| = 11.5 Hz, 8H), 3.63-3.68 (m, 4H), 7.11 (s, 6H), 7.22 (s, 2H); ^{13}C NMR (CDCl$_3$ with drops of CD$_3$OD, 75 MHz) δ (ppm) 22.5, 22.8, 24.8, 25.2, 32.7, 42.6, 52.6, 52.9, 61.0, 129.1, 137.8, 175.2; ESI TOF MS (m/z) 885.6 [(M+H)$^+$, 100], 908.7 [(M+Na)$^+$, 95], 454.3 [(M+H+Na)$^{2+}$, 45].

Compund 3f: This compound was obtained as described above starting from **1f** and therephthaldehyde, and was characterized as free amine. Yield = 41%; white solid; M.P.= It decomposes without melting over 290 ºC; [α]$_D^{20}$ = +17.68 (c = 0.90, CHCl$_3$:CH$_3$OH 7:3); IR (cm^{-1}) (KBr) 3294, 3056, 3011, 2933, 2857, 1655, 1522; ^{1}H NMR (CDCl$_3$, CD$_3$OD, 500 MHz) δ (ppm) 0.75 (t, J = 7.3 Hz, 12H), 0.78 (d, J = 6.8 Hz, 12H), 0.91-1.01 (m, 4H), 1.13-1.27 (m, 8H), 1.34-1.42 (m, 4H), 1.60-1.66 (m, 8H), 2.02 (d, J = 12.5 Hz, 4H), 2.84 (bs, 4H), 3.23-3.27 (m, 4H, overlapped with solvent signal), 3.37 (ABq, δ_A = 3.44, δ_B = 3.30, |J_{AB}| = 11.6 Hz, 8H), 3.60-3.62 (m, 4H), 6.95 (s, 8H); ^{13}C NMR (CDCl$_3$, CD$_3$OD, 75 MHz) δ (ppm) 11.5, 15.1, 24.4, 25.5, 32.5, 37.7, 52.4, 52.6, 66.7, 128.7, 137.2, 173.7; ESI TOF MS (m/z) 885.6 [(M+H)$^+$, 100], 907.6 [(M+Na)$^+$, 70], 443.3 [(M+2H)$^{2+}$, 65], 454.8 [(M+H+Na)$^{2+}$, 50].

Compound 3g: This compound was obtained as described above starting from **1g** and therephthaldehyde. To avoid deprotection of the side chain the reduction was hydrolyzed with a 1M aqueous solution of ammonium acetate. Yield = 17%; white solid; M.P.= 173-178 ºC; [α]$_D^{20}$ = +4.06 (c = 1.20, CHCl$_3$); IR (cm^{-1}) (KBr) 3315, 3057, 2931, 2857, 1803, 1513; ^{1}H NMR (CD$_3$OD, 500 MHz) δ (ppm) 1.23-1.38 (m, 12H), 1.66-1.75 (m, 8H), 1.78-1.85 (m, 4H), 2.03 (d, J = 11.5 Hz, 4H), 2.25-2.32 (m, 4H), 2.35-2.41 (m, 4H), 3.04 (t, J = 6.6 Hz, 4H), 3.42 (ABq, δ_A = 3.52, δ_B = 3.32, |J_{AB}| = 14.6 Hz, 8H), 3.65-3.67(m, 4H), 7.02 (s, 8H), 7.17-7.24 (m, 60H); ^{13}C NMR (CD$_3$OD, 125 MHz) δ (ppm) 24.6, 29.4, 32.4, 32.9, 52.0, 52.6, 61.5, 70.4, 126.6, 127.5, 128.5, 128.8, 138.3, 144.8, 173.3, 175.2; ESI TOF MS (m/z) 639.0 [(M+3H)$^{3+}$, 100], 957.9 [(M+2H)$^{2+}$, 90].

Compound 5a: Bis(amidoamine) **1c** (50.5 mg, 0.1616 mmol) was disolved in 3 mL of degassed CH$_3$OH, the solution was placed inside a flask under nitrogen. Freshly distilled benzaldehyde (33 µL, 0.3232 mmol) was dissolved in 200 µL of degassed CH$_3$OH, this solution was added over the solution of **1c** (0.05 M final concentration **1c**). The mixture was stirred overnight and the solvent was evaporated in vacuum. The obtained compound showed high purity by NMR and was used without further purification. Yield = quantitative; white solid; M.P.= 172-176 ºC; [α]$_D^{20}$ = –25.57 (c = 1.08, CHCl$_3$); IR (cm^{-1}) (KBr) 3280, 3062, 2959, 2931, 2856, 1643, 1533; ^{1}H NMR (CDCl$_3$) δ (ppm) 0.91 (d, J = 6.8 Hz, 6H), 0.94 (d, J = 6.8 Hz, 6H), 1.11-1.19 (m, 2H), 1.26-1.33 (m, 2H), 1.66-1.67 (m, 2H), 2.12 (bs, 1H), 2.15 (bs, 1H), 2.31-2.38 (m, 2H), 3.56 (d, J = 5.0 Hz, 2H), 3.71-3.75 (m, 2H), 6.99 (bd, J = 6.1 Hz, 2H), 7.43-7.47 (m, 6H), 7.81 (dd, J_1 = 7.2 Hz, J_2 = 2.3 Hz, 4H), 8.14 (s, 2H); ^{13}C NMR (CDCl$_3$, 125 MHz) δ (ppm) 18.4, 20.0, 24.8, 32.6, 32.8, 53.2, 80.1, 128.8, 128.9, 131.3, 135.9, 162.3, 173.3; ESI TOF MS (m/z) 489.3 [(M+H)$^+$, 100], 511.3 [(M+Na)$^+$, 90].

Compound 5b: This compound was obtained as described above starting from **1h** and benzaldehyde but the mixture was stirred at R. T. for 3 days. Yield = 93%; white solid; M.P.= 149-155 ºC; [α]$_D^{20}$ = –126.21 (c = 0.93, CHCl$_3$:MeOH 9:1); IR (cm^{-1}) (KBr) 3305, 3063, 2960, 2933, 2859, 1645, 1537; ^{1}H NMR (CDCl$_3$) δ (ppm) 0.77 (d, J = 6.9 Hz, 6H), 0.83 (d, J = 6.9 Hz, 6H), 1.27-1.42 (m, 4H), 1.74-1.76 (m, 2H), 2.09-2.14 (m, 2H), 2.17 (bs, 1H), 2.19 (bs, 1H), 3.14 (d, J = 4.6 Hz, 2H), 3.70-3.75 (m, 2H), 6.81 (bd, J = 5.7 Hz, 2H), 7.44-7.46 (m, 6H), 7.56 (s, 2H), 7.64-7.66 (m, 4H); ^{13}C NMR (CDCl$_3$, 125 MHz) δ (ppm) 17.7, 19.5, 25.0, 32.8, 32.9, 52.9, 79.6, 128.8, 128.8, 131.3, 135.7, 161.8, 172.9; ESI TOF MS (m/z) 489.23 [(M+H)$^+$, 100], 511.24 [(M+Na)$^+$, 50].

Compound 5c: This compound was obtained as described above starting from **1a** and benzaldehyde. Yield = quantitative; white solid; M.P.= 124-129 ºC; [α]$_D^{20}$ = +82.45 (c = 1.05, CHCl$_3$); IR (cm^{-1}) (KBr) 3378, 3341, 2963, 2930, 2867, 2846, 2819, 1651, 1519; ^{1}H NMR (CDCl$_3$) δ (ppm) 0.89 (d, J = 6.8 Hz, 6H), 0.94 (d, J = 6.8 Hz, 6H), 2.30-2.36 (m, 2H), 3.39-3.46 (m, 2H), 3.48-3.55 (m, 2H), 3.58 (d, J = 3.9 Hz, 2H), 7.11 (bs, 2H), 7.42-7.47 (m, 6H), 7.77 (d, J = 6.6 Hz, 4H), 8.06 (s, 2H); ^{13}C NMR (CDCl$_3$, 125 MHz) δ (ppm) 17.6, 19.8, 33.1, 39.3, 79.2, 128.7, 128.9, 131.4, 135.7, 162.5, 173.6; ESI TOF MS (m/z) 457.22 [(M+Na)$^+$, 100], 435.28 [(M+H)$^+$, 80], 473.25 [(M+K)$^+$, 50].

Compound 5d: This compound was obtained as described above starting from the D,D enantiomer of **1a** and benzaldehyde. It showed spectroscopic data identical to **5c**, as expected for enantiomers. Yield = quantitative; white solid; M.P.= 132-136 ºC; [α]$_D^{20}$ = –91.39 (c = 0.99, CHCl$_3$).

Acknowledgements

[1] For some recent examples: a) S. E. Gibson, C. Lecci, *Angew. Chem.* **2006**, *118*, 1392–1405; *Angew. Chem. Int. Ed.* **2006**, *45*, 1364–1377; b) L. A. Wessjohann, B. Voigt, D. G. Rivera, *Angew. Chem.* **2005**, *117*, 4863–4868; *Angew. Chem., Int. Ed.* **2005**, *44*, 4785–4790.

[2] For some examples on related systems: (a) K. Choi, A. D. Hamilton *Coord. Chem Rev.* **2003**, *240*, 101–110; b) K. Choi, A. D. Hamilton *J. Am. Chem. Soc.* **2003**, *125*, 10241–10249; c) K. Choi, A. D. Hamilton *J. Am. Chem. Soc.* **2001**, *123*, 2456–2457; d) L. Somogyi, G. Haberhauer, J. Rebek, Jr. *Tetrahedron* **2001**, *57*, 1699–1708; e) M. M. Conn, J. Rebek, Jr. *Chem. Rev.* **1997**, *97*, 1647–1668.

[3] a) L. Gentilucci, A. Tolomelli, F. Squassabia *Curr. Med. Chem.* **2006**, *13*, 2449–2466; b) C. T. Walsh *Science* **2004**, *303*, 1805–1810. c) W. A. Loughlin, J. D. A. Tyndall, M. P. Glenn, D. P. Fairlie *Chem. Rev.* **2004**, *104*, 6085–6117; d) R. C. Reid, L. K. Pattenden, J. D. A. Tyndall, J. L. Martin, T. Walsh, D. P. Fairlie *J. Med. Chem.* **2004**, *47*, 1641–1651; e) R. C. Reid, G. Abbenante, S. M. Taylor, D. P. Fairlie *J. Org. Chem.* **2003**, *68*, 4464–4471; f) X. Hu, K. T. Nguyen, C. L. M. J. Verlinde, W. G. J. Hol, D. Pei *J. Med. Chem.* **2003**, *46*, 3771–3774; g) S. Fernández-López, H.-S. Kim, E. C. Choi, M. Delgado, J. R. Granja, A. Khasanov, K. Kraehenbuehl, G. Long, D. A. Weinberger, K. M. Wilcoxen, M. R. Ghadiri *Nature* **2001**, *412*, 452–455; h) D. P. Fairlie, G. Abbenante, D. R. March *Curr. Med. Chem.* **1995**, *2*, 654–686.

[4] a) R. J. Brea, L. Castedo, J. R. Granja, *Chem. Commun.* **2007**, 3267–3269; b) N. Ashkenasy, S. W. Horn, M. R. Ghadiri *Small* **2006**, *2*, 99–102; c) W. S. Horne, C. D. Stout, M. R. Ghadiri, *J. Am. Chem. Soc.* **2003**, *125*, 9372–9376; c) D. T. Bong, T. D. Clark, J. R. Granja, M. R. Ghadiri *Angew. Chem.* **2001**, *113*, 2221-2224; *Angew. Chem. Int. Ed. Engl.* **2001**, *40*, 988–1011; (d) D. Ranganthan *Acc. Chem. Res.* **2001**, *34*, 919–930.

[5] a) K. Gloe *Macrocyclic Chemistry: Current Trends and Future Perspectives*, Springer, Dordrecht, **2005**; b) D. Parker, *Macrocycle Synthesis: A Practical Approach*, Oxford University Press, New York, **1996**; c) B. Dietrich, P. Viout, J.-M. Lehn *Macrocyclic Chemistry*, VCH, New York, **1993**; d) F. Vögtle *Cyclophane Chemistry*, Wiley, Chichester, **1993**; e) N. Sokolenko, G. Abbenante, M. J. Scanlon, A. Jones, L. R. Gahan, G. R. Hanson, D. P. Fairlie, *J. Am. Chem. Soc.* **1999**, *121*, 2603–2604.

[6] a) S. B. Y. Shin, B. Yoo, L. J. Todaro, K Kirshenbaum *J. Am. Chem. Soc.* **2007**, *129*, 3218–3225; c) D. G. Rivera, L. A. Wessjohann *J. Am. Chem. Soc.* **2006**, *128*, 7122–7123; d) H. Jiang, J.-M. Léger, P. Guionneau, I. Huc *Org. Lett.* **2004**, *6*, 2985–2988; e) T. Velasco-Torrijos, P. V. Murphy *Org. Lett.* **2004**, *6*, 3961–3964; f) T. V. R. S. Sastry, B. Banerji, S. K. Kumar, A. C. Kunwar, J. Das, J. P. Nandy, J. Iqbal *Tetrahedron Lett.* **2002**, *43*, 7621–7625.

[7] a) M. Amorín, L. Castedo, J. R. Granja *Chem. Eur. J.* **2008**, *14*, 2100–2111; b) M. Sastry, C. Brown, G. Wagner, T. D. Clark. *J. Am. Chem. Soc.* **2006**, *128*, 10650–10651; c) Z.-T. Li, J.-L. Hou, C. Li, H.-P. Yi *Chem. Asian J.* **2006**, *1*, 766-778; d) R. P. Cheng *Curr. Opin. Struct. Biol.* **2004**, *14*, 512-520.

[8] a) N. Delsuc, J.-M. Léger, S. Massip, I. Huc *Angew. Chem.* **2007**, *119*, 218-221; *Angew. Chem. Int. Ed.* **2007**, *46*, 214-217. b) R. Gray, J. O. Trent *Biochemistry* **2005**, *44*, 2469-2477; c) M. Jourdan, M. S. Searle *Biochemistry* **2001**, *40*, 10317-10325.

[9] a) P. Cintas *Angew. Chem.* **2002**, *114*, 1187-1193; *Angew. Chem. Int. Ed.* **2002**, *41*, 1139-1145; b) J. L. Bada *Nature*, **1995**, *374*, 594-595; c) W. A. Bonner, *Origins Life Evol. Biosph.* **1991**, *21*, 59-111.

[10] a) W. C. Pomerantz, V. M. Yuwono, C. L. Pizzey, J. D. Hartgerink, N. L. Abbot, S. H. Gellman *Angew. Chem.* **2008**, *120*, 1261–1264; *Angew. Chem Int. Ed.* **2008**, *47*, 1241–1244; b) W. S. Horne, J. L. Price, J. L. Keck, S. H. Gellman *J. Am. Chem. Soc.* **2007**, *129*, 4178–4180; c) T. A. Martinek, A. Hetényi, L. Fülöp, I. M. Mádity, G. K. Tóth, I. Dékány, F. Fülöp *Angew. Chem.* **2006**, *118*, 2456–2460; *Angew. Chem. Int. Ed.* **2006**, *45*, 2396–2400; d) C. Tomasini, G. Luppi, M. Monari *J. Am. Chem. Soc.* **2006**, *128*, 2410–2420; e) A. I. Jimenez, G. Ballano, C. Cativiela *Angew. Chem.* **2005**, *117*, 400–402; *Angew. Chem. Int. Ed.* **2005**, *44*, 396–399; f) C. Dolain, H. Jiang, J.-M. Léger, P. Guinneau, I. Huc. *J. Am. Chem. Soc.* **2005**, *127*, 12943–12951; g) D. Yang, J. Qu, W. Li, D.-P. Wang, Y. Ren, Y.-D. Wu *J. Am. Chem. Soc.* **2003**, *125*, 14452–14457; h) A. I. Jiménez, C. Cativiela, J. Gómez-Catalán, J. J. Pérez, A. Aubry, M. París, M. Marraud *J. Am. Chem. Soc.* **2000**, *122*, 5811–5821.

[11] For some reviews on foldamers, see: a) M. T. Stone, J. M. Heemstra, J. S. Moore *Acc. Chem. Res.* **2006**, *39*, 11–20; b) G. Licini, L. J. Prins, P. Scrimin *Eur. J. Org. Chem.* **2005**, 969–977; c) I. Huc *Eur. J. Org. Chem.* **2004**, 17–29; b) R. P. Cheng, S. H. Gellman, W. F. DeGrado, *Chem. Rev.* **2001**, *101*, 3219-3232; c) D. J. Hill, M. J. Mio, R. B. Prince, T. S. Hughes, J. S. Moore *Chem. Rev.* **2001**, *101*, 3893–4011; d) M. S. Cubberley, B. L. Iverson *Curr. Opin. Chem. Biol.* **2001**, *5*, 650–653; e) S. H. Gellman, *Acc. Chem. Res.* **1998**, *31*, 173–180. (b) D. Seebach, J. L. Matthews *J. Chem. Soc., Chem. Commun.* **1997**, 2015–2022.

[12] For a recent review, see: J. Blankenstein, J. Zhu, *Eur. J. Org. Chem.* **2005**, 1949–1964.

[13] a) J. M. Holub, H. J. Jang, K. Kirshenbaum *Org. Lett.* **2007**, *9*, 3275–3278; b) F. Campbell, J. Plante, C. Carruthers, M. J. Hardie, T. J. Prior, A. J. Wilson *Chem. Commun.* **2007**, 2240–2242; c) X. Bu, X. Wu, N. L. J. Ng, C. K. Mak, C. Qin, Z. Guo, *J. Org. Chem.* **2004**, *69*, 2681–2685; d) W. Jiang, J. Wanner, R. J. Lee, P. Y. Bounaud, D. L. Boger *J. Am. Chem. Soc.* **2003**, *125*, 1877–1887; e) X. Bu, X. Wu, G. Xie, Z. Guo *Org. Lett.* **2002**, *4*, 2893-2895; f) T. D. Clark, M. R. Ghadiri *J. Am. Chem. Soc.* **1995**, *117*, 12364–12365.

[14] a) W. T. Gong, K. Hiratani, T. Oba, S. Ito *Tetrahedron Lett.* **2007**, *48*, 3073–3076.; b) A. Zhang, Y. Han, K. Yamato, X. C. Zeng, B. Gong *Org. Lett.* **2006**, *8*, 803–806.; c) C. Rotger, M. N. Pina, M. Vega, P. Ballester, P. M. Deya, A. Costa *Angew. Chem.* **2006**, *118*, 6998-7002; *Angew. Chem. Int. Ed.* **2006**, *45*, 6844–6848.; d) L. Yuan, W. Feng, K. Yamato, A. R. Sanford, D. Xu, H. Guo, B. Gong *J. Am. Chem. Soc.* **2004**, *126*, 11120–11121.; e) M. C. Rotger, M. N. Pina, A. Frontera, G. Martorell, P. Ballester, P. M. Deya, A. Costa *J. Org. Chem.* **2004**, *69*, 2302–2308; f) F. J. Carver, C. A. Hunter, R. J. Shannon *J. Chem. Soc., Chem. Commun.* **1994**, 1277–1280.

[15] a) C. Peña, I. Alfonso, V. Gotor *Eur. J. Org. Chem.* **2006**, 3887-3897; b) J. E. W. Scheuermann, K. F. Sibbons, D. M. Benoit, M. Motevalli, M. Watkinson *Org. Biomol. Chem.* **2004**, *2*, 2664–2670.; c) G. Stones, G. Argouarch, A. R. Kennedy, D. C. Sherrington, C. L. Gibson *Org. Biomol. Chem.* **2003**, *1*, 2357–2363.; d) B. Altava, M. I. Burguete, B. Escuder, S. V. Luis, E. García-España, M. C. Muñoz *Tetrahedron* **1997**, *53*, 2629-2640; e) J. E. Richman, T. J. Atkins *J. Am. Chem. Soc.* **1974**, *96*, 2268–2270.

[16] a) D. Zhao, J. S. Moore *J. Org. Chem.* **2002**, *67*, 3548–3554; b) R. A. Abramovitch, X. Ye, W. T. Pennington, G. Schimek, D. Bogdal *J. Org. Chem.* **2000**, *65*, 343–351.; c) R. A. Abramovitch, X. Ye *J. Org. Chem.* **1999**, *64*, 5904–5912

[17] A. Saghatelian, Y. Yokobayashi, K. Soltani, M. R. Ghadiri *Nature*, **2001**, *409*, 797–801.

[18] J. Becerril, M. Bolte, M. I. Burguete, F. Galindo, E. García-España, S. V. Luis, J. F. Miravet, *J. Am. Chem. Soc.* **2003**, *125*, 6677–6686.

[19] a) J. Becerril, B. Escuder, J. F. Miravet, R. Gavara, S. V. Luis, *Eur. J. Org. Chem.* **2005**, 481–485; b) J. Becerril, M. I. Burguete, B. Escuder, F. Galindo, R. Gavara, J. F. Miravet, S. V. Luis, G. Peris, *Chem. Eur. J.* **2004**, *10*, 3879–3890; c) J. Becerril, M. I. Burguete, B. Escuder, S. V. Luis, J. F. Miravet, M. Querol *Chem. Commun.* **2002**, 738–739.

[20] I. Alfonso, M. I. Burguete, S. V. Luis, J. F. Miravet, P. Seliger, E. Tomal, *Org. Biomol. Chem.* **2006**, *4*, 853–859.

[21] a) M. I. Burguete, F. Galindo, M. A. Izquierdo, S. V. Luis, L. Vigara, *Tetrahedron* **2007**, *63*, 9493–9501; b) M. I. Burguete, F. Galindo, S. V. Luis, L. Vigara *Dalton Trans.* **2007**, 4027–4033; c) F. Galindo, M. I. Burguete, L. Vigara, S. V. Luis, D. A. Russell, N. Kabir, J. Gavrilovic, *Angew. Chem.* **2005**, *117*, 6662–6666; *Angew. Chem. Int. Ed.* **2005**, *44*, 6504–6508; d) F. Galindo, J. Becerril, M. I. Burguete, S.V. Luis, L. Vigara, *Tetrahedron Lett.* **2004**, *45*, 1659–1662.

[22] a) I. Alfonso, M. I. Burguete, F. Galindo, S. V. Luis, L. Vigara *J. Org. Chem.* **2007**, *72*, 7947–7956; b) I. Alfonso, M. I. Burguete, S. V. Luis, *J. Org. Chem.* **2006**, *71*, 2242–2250.

[23] N. E. Borisova, M. D. Reshetova, Y. A. Ustynyuk *Chem. Rev.* **2007**, *107*, 46–79.

[24] a) I. Alfonso, M. Bolte, M. Bru, M. I. Burguete, S. V. Luis, J. Rubio *J. Am. Chem. Soc.* **2008**, *130*, 6137–6144; b) M. Bru, I. Alfonso, M. I. Burguete, S. V.

Luis *Angew. Chem.* **2006**, *118*, 6301–6305; *Angew. Chem. Int. Ed.* **2006**, *45*, 6155–6159.

[25] M. Bru, I. Alfonso, M. I. Burguete, S. V. Luis, *Tetrahedron Lett.* **2005**, *46*, 7781–7785.

[26] a) J. Gawroński, M. Kwit, J. Grajewski, J. Gajewy, A. Dlugokinska *Tetrahedron: Asymmetry* **2007**, *18*, 2632–2637.; b) M. Kwit, A. Plutecka, U. Rychlewska, J. Gawroński, A. F. Khlebnikov, S. I. Kozhushkov, K. Rauch, A. De Meijere *Chem. Eur. J.* **2007**, *13*, 8688–8695; c) J. Gawroński, K. Gawronska, J. Grajewski, M. Kwit, A. Plutecka, U. Rychlewska, *Chem. Eur. J.* **2006**, *12*, 1807–1817; d) N. Kuhnert, A. M. Lopez-Periago, G. M. Rossignolo, *Org. Biomol. Chem.* **2005**, *3*, 524–537; e) N. Kuhnert, N. Burzlaff, C. Patel, A. Lopez-Periago, *Org. Biomol. Chem.* **2005**, *3*, 1911–1921; f) J. Gawroński, M. Brzostowska, M. Kwit, A. Plutecka, U. Rychlewska, *J. Org. Chem.* **2005**, *70*, 10147–10150; g) N. Kuhnert, G. M. Rossignolo, A. M. Lopez-Periago, *Org. Biomol. Chem.* **2003**, *1*, 1157–1170; h) N. Kuhnert, C. Straßnig, A. M. Lopez-Periago, *Tetrahedron: Asymmetry* **2002**, *13*, 123–128; i) M. Chadim, M. Buděšinsky, J. Hodačova, J. Zavada, P. C. Junk, *Tetrahedron: Asymmetry* **2001**, *12*, 127–133; J. Gawroński, H. Kołbon, M. Kwit, A. Katrusiak, *J. Org. Chem.* **2000**, *65*, 5768–5773.

[27] a) A. González-Álvarez, I. Alfonso, V. Gotor *Chem. Commun.* **2006**, 224–226; b) A. González-Álvarez, I. Alfonso, F. López-Ortiz, A. Aguirre, S. García-Granda, V. Gotor *Eur. J. Org. Chem.* **2004**, 1117–1127.

[28] a) S. Hanessian, V. Vinci, K. Fettis, T. Maris, M. T. P. Viet *J. Org. Chem.* **2008**, *73*, 1181–1191; b) C. Peña, I. Alfonso, B. Tooth, N. H. Voelcker, V. G. Gotor *J. Org. Chem.* **2007**, *72*, 1924–1930.

[29] a) N. Berova, L. Di Bari, G. Pescitelli, *Chem. Soc. Rev.* **2007**, *36*, 914–931; b) N. Berova, K. Nakanishi, R. W. Woody, *Circular Dichroism. Principles and Applications*, Wiley-VCH, **2000**, New York.

[30] M. Kaik, J. Gawroński, *Org. Lett.* **2006**, *8*, 2921–2924.

[31] An experimental support for this hypothesis can be obtained from the NMR data of **1c** and **1h** in CDCl₃ (see Supporting Information). The chemical shifts of the amide NH protons are 7.25 ppm and 7.36 ppm for **1c** and **1h**, respectively. This suggests a larger H-bonded character of that proton in **1h**. We thank the suggestion of an anonymous referee who prompted us to revise these data.

[32] a) N. J. Greenfield *Anal. Biochem.* **1996**, *235*, 1–10; b) A. Percze1, M. Hollósi, B. M. Foxman, G. D. Fasman *J. Am. Chem. Soc.* **1991**, *113*, 9772–9184.

[33] L. You, R. Ferdani, R. Li, J. P. Kramer, R. E. K. Winter, G. W. Gokel *Chem. Eur. J.* **2008**, *14*, 382–396, and references therein.

[34] E. Gouaux, R. MacKinnon *Science* **2005**, *310*, 1461–1465.

[35] R.H. Blessing *Acta Crystallogr. Sect. A* **1995**, *51*, 33–38.

[36] G.M. Sheldrick *Acta Crystallogr. Sect. A* **2008**, *64*, 112–122.

Chirality induced correct folding for macrocyclization

Ignacio Alfonso,* Michael Bolte, Miriam Bru, M. Isabel Burguete, and Santiago V. Luis.*

Designed folding of pseudopeptides: the transformation of a configurationally driven preorganization into a stereoselective multicomponent macrocyclization
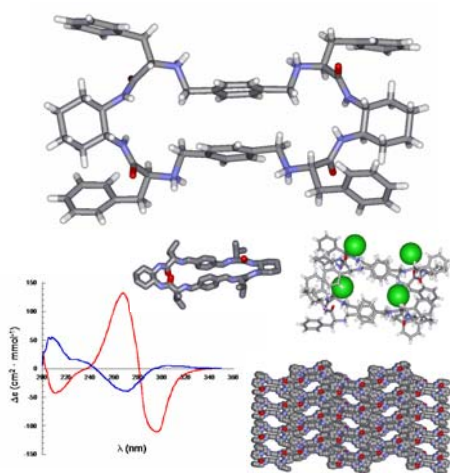
An efficient [2+2] reductive amination macrocyclization is governed by the stereochemical information contained in the corresponding linear precursors, as demonstrated by NMR, CD and modeling studies with both the macrocyclic imine intermediates and the corresponding open-chain model compounds. Crystal structure of the HCl salt of one macrocycle shows the formation of hydrophobically embedded chloride channels.